Journal of Fluorescence (2019) 29:1457–1465
https://doi.org/10.1007/s10895-019-02451-8

ORIGINAL ARTICLE

# Fluorescence Imaging of Mitochondria with Three Different Sets of Signals Based on Fluorene Cation Fluorescent Probe

Weishan Wang[1] · Yong Liu[1] · Jie Niu[1] · Weiying Lin[1]

Received: 22 July 2019 / Accepted: 1 October 2019 / Published online: 26 November 2019
© Springer Science+Business Media, LLC, part of Springer Nature 2019

## Abstract

Herein, we develop a novel mitochondria-targetable fluorescence probe (**FVPI**) based on fluorene cation derivative. This mitochondria-targetable fluorescence probe exhibits large Stokes shift in various solutions. In addition, **FVPI** displays numerous advantages, including high photostability, low cytotoxicity, and two-photon properties. View of the above features, **FVPI** is successfully capable of imaging mitochondria in biological systems with three different sets of signals. This finding will provide a new platform for the constructing mitochondria-targetable fluorescent probes with excellent optical properties.

**Keywords** Tracking · Fluorene derivative · Large stokes shift · Mitochondria · Three signals · Zebrafish

## Introduction

The mitochondria with membrane structure is closely linked to important signal transduction in the process of physiological activities [1–4]. It is the location for cell respirations, including Krebs cycle and oxidation-phosphorylation system. Mitochondria could produce ATP to meet the bioenergetic requirements of cells by oxidation-phosphorylation system [5, 6]. In addition, mitochondria also play an important role in other types of metabolism, such as regulating the dynamic balance of $Ca^{2+}$ concentration and synthesizing and iron-sulfur protein [7–11]. Therefore, mitochondrial metabolism is associated with a large number of diseases, such as arteriosclerosis, Parkinson's disease, heart disease and cancer [12–17]. Thus, in order to understand the physiological function of mitochondria, it is very necessary to visually monitor mitochondria.

The fluorescence probes techniques provide powerful tools for tracking dynamic process of organelles [18–23]. Stokes shift is an important index to evaluate fluorescence probe that could accurately locate target analyses in living cells [24]. The fluorescence probe with large Stokes shift is capable of eliminating images error and locating the target accurately in living biological systems [25–30]. Therefore, it is important to construct fluorescent probe with a large Stokes shift. Up to now, numerous investigations in the past decade have focused on developing mitochondria–targetable fluorescent probes in related fields [31–39]. Although many mitochondria probes have been used as commercial dyes, these probes exhibited few Stokes shift in diverse solutions [40, 41]. Especially, fluorescent probes which could located at mitochondria with large Stokes shift are still rare [42]. Therefore, it is crucial to develop a innovative fluorescent probe with large Stokes shift for tracking mitochondria with three emission colors.

Herein, we construct a mitochondria-targetable fluorescence probe (**FVPI**) based on fluorene cation derivative (Fig. 1). The probe could successfully track mitochondria with three emission colors. Moreover, it not only exhibits a large Stokes shift in various solutions, but also possesses a series of advantages, including high photostability, low cytotoxicity, and two-photon properties. View of this, this probe **FVPI** could track mitochondria in the in living system with three different sets of signals.

**Electronic supplementary material** The online version of this article (https://doi.org/10.1007/s10895-019-02451-8) contains supplementary material, which is available to authorized users.

✉ Weiying Lin
weiyinglin2013@163.com

[1] Institute of Fluorescent Probes for Biological Imaging, School of Materials Science and Engineering, School of Chemistry and Chemical Engineering, University of Jinan, Shandong 250022, People's Republic of China

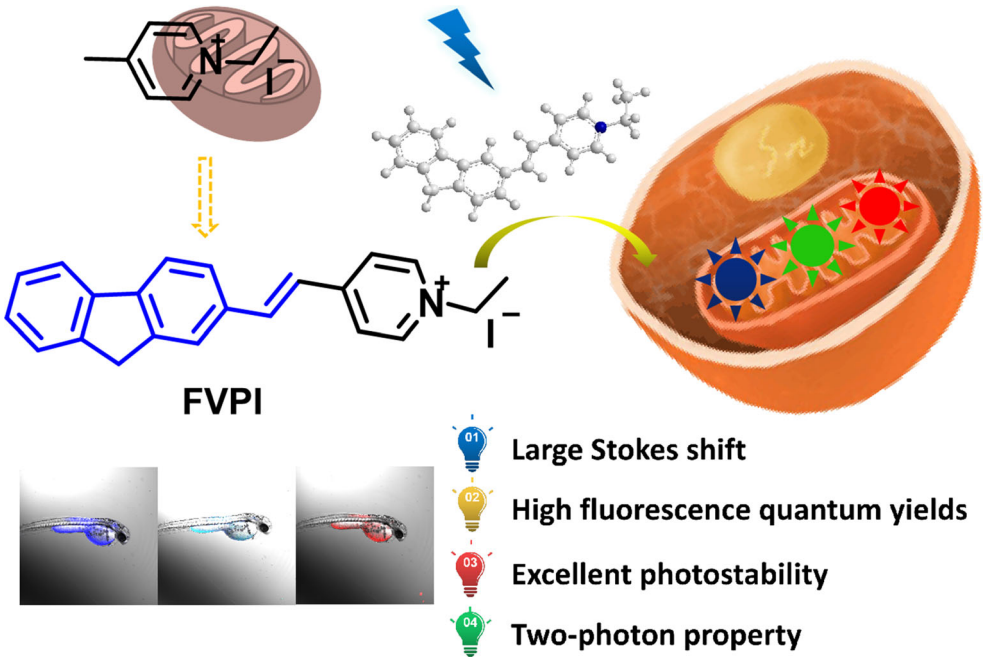


**Fig. 1** Design of the probe **FVPI** for target mitochondria

## Experimental Section

### Synthesis

*Synthesis of compound 3:* Bromofluorene (1.0 g, 4.07 mmol), tri-(o-tolyl) phosphine (0.25 g, 0.81 mmol), palladium (II) acetate (91.58 mg, 0.407 mmol) were introduced into dry TEA/DMF (45 mL, *v*/v = 2:1) mixed solvent, the reaction solution was stirred under argon for 20 min at 25 °C (Scheme 1). Then, 4-Vinylpyridine (1.2 g, 12.21 mmol) was added. Under the protection of argon, the reaction mixture was heated up to 95 °C and kept at this temperature in an oil bath for 48 h. The resulting mixture was allowed to cool to room temperature, and TEA was removed in vacuo. The mixture was extracted with $CH_2Cl_2$ and $H_2O$, then dried over anhydrous magnesium sulfate, the solution was concentrated under reduced pressure. The residue was purified by column chromatography with petroleum ether/ethyl acetate (2:1) as eluent to give the pale yellow product with a yield of 40%. $^1$H NMR (400 MHz, $CDCl_3$) $\delta$ 8.59 (d, $J$ = 4.0 Hz, 2H), 7.80 (d, $J$ = 8.0 Hz, 2H), 7.75 (s, 1H), 7.57 (d, $J$ = 4.0 Hz, 2H), 7.33–7.41 (m, 5H), 7.09 (d, $J$ = 16.0 Hz, 1H), 3.94 (s, 2H).

*Synthesis of **FVPI**:* Compound 3 (0.30 g, 1.1 mmol) and Iodoethane (0.34 g, 2.2 mmol) were dissolved in the 20 mL of EtOH. Under the protection of argon, the solution was stirred at 80 °C for 20 h. The resulting mixture was allowed to cool to room temperature, and solution was removed under reduced pressure.. The crude purified by silica column chromatography ($CH_2Cl_2$ / $CH_3OH$ (10:1, *v*/v)) to give the yellow product with a yield of 65%. $^1$H NMR (400 MHz, DMSO-$d_6$) $\delta$ 8.99 (d, $J$ = 8.0 Hz, 2H), 8.27 (d, $J$ = 8.0 Hz, 2H), 8.16 (d, $J$ = 16.0 Hz, 1H), 8.02 (m, 3H), 7.80 (d, $J$ = 8.0 Hz, 1H), 7.63 (t, $J$ = 12.0 Hz, 2H), 7.42 (m, 2H), 4.55 (q, $J$ = 6.0 Hz, 2H), 4.03 (s, 2H), 1.54 (t, $J$ = 8.0 Hz, 3H). $^{13}$C NMR (100 MHz, DMSO-$d_6$) $\delta$ 153.38, 144.41, 144.32, 143.93, 141.63, 140.80, 140.77, 134.28, 128.26, 128.10, 127.47, 127.23, 125.76, 124.93, 124.14, 122.95, 121.13, 121.07, 55.67, 49.07, 36.81, 16.66. HRMS (m/z): $[M\text{-}I]^+$ calcd for $C_{22}H_{20}N^+$: 298.1590, found, 298.1563.

### Apparatus and Chemicals

Bromofluorene, tri- (o-tolyl) phosphine, palladium (II) acetate and Iodoethane were bought from commercial suppliers (Energy Chemical). Analytical reagents used in synthesis experiments not need to further purification. Unless otherwise indicated; Thin-Layer Chromatography (TLC) used to monitoring organic experimental process. Furthermore, isolation and depuration of products were performed by column chromatography; The company (Qingdao Ocean Chemicals)

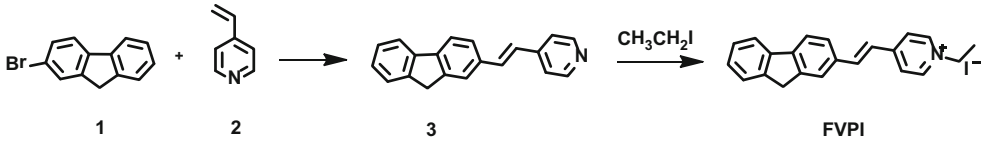


**Scheme 1** The synthetic route to the probe **FVPI.**

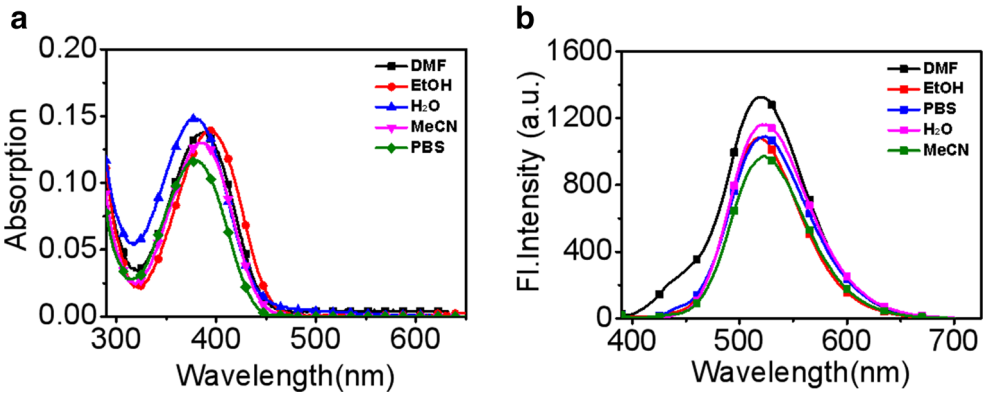


**Fig. 2** (A) Absorption spectra and (B) fluorescence responses of **FVPI** toward diverse solvents. [**FVPI**]: 10 μM

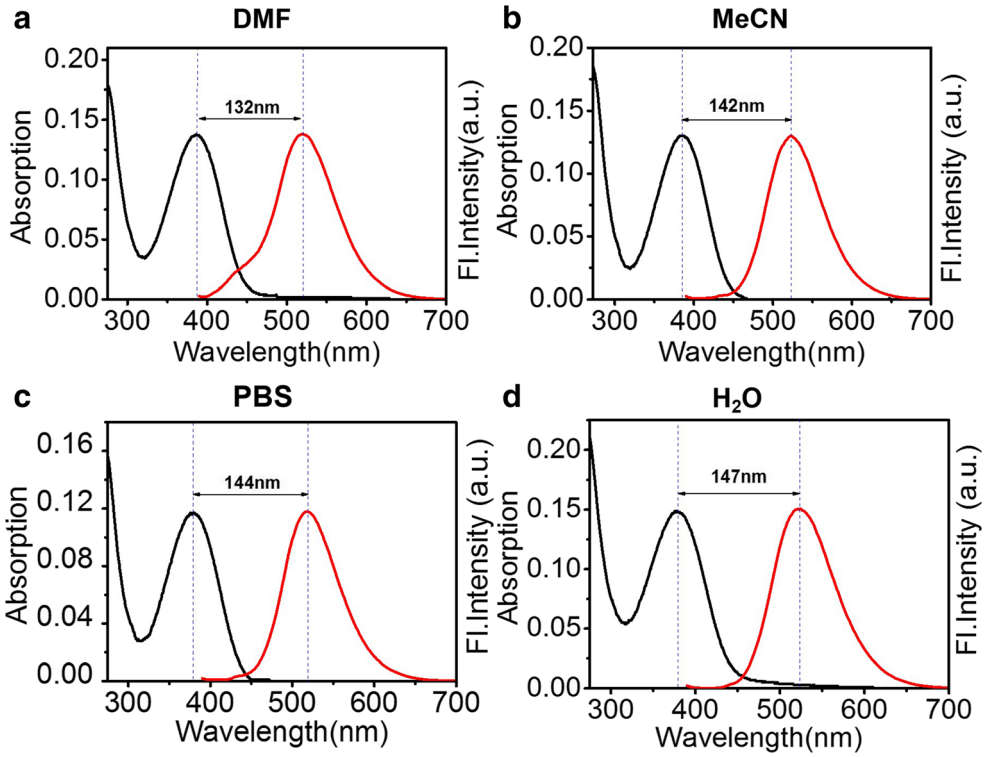


**Fig. 3** (A) The UV (black) and FL spectra (red) in DMF of the probe; (B) The UV (black) and FL spectra (red) in MeCN of the probe; (C): The UV (black) and FL spectra (red) in PBS of the probe; (D): The UV (black) and FL spectra (red) in $H_2O$ of the probe. [**FVPI**]: 10 μM

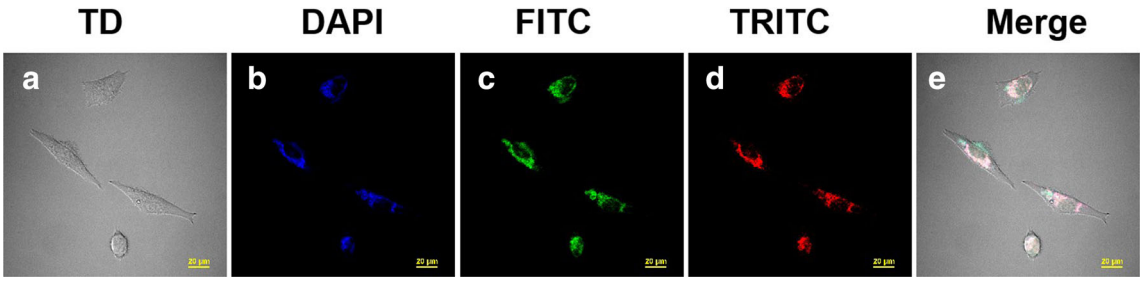


**Fig. 4** Confocal microscopy images of of HeLa cells treated with **FVPI** (10 mM) for 30 min.(A) Bright-field image; (B) The blue emission channel ($\lambda_{ex}$ = 405 nm, $\lambda_{em}$ = 425–475 nm); (C) The green emission channel ($\lambda_{ex}$ = 405 nm, $\lambda_{em}$ = 500–550 nm); (D) The red emission channel ($\lambda_{ex}$ = 405 nm, $\lambda_{em}$ = 570–620 nm); (E) merged image. Scale bar = 20 μm

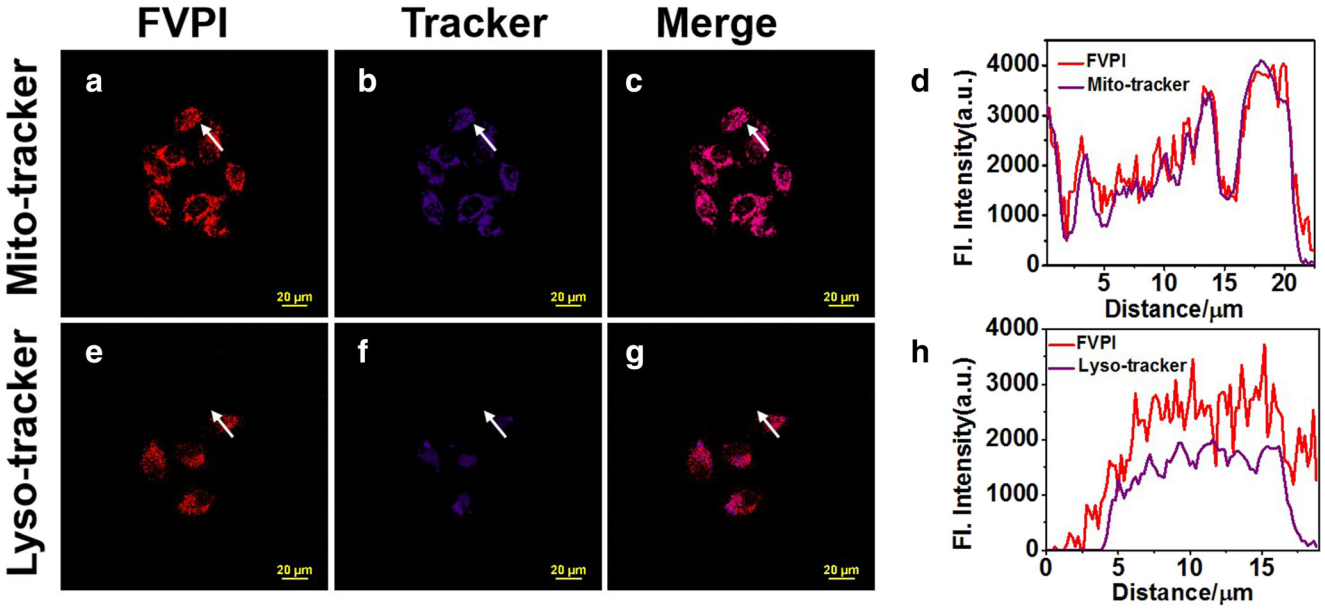


**Fig. 5** Fluorescence image of HeLa cells treated with **FVPI** (10 μM) for 30 min and commercial organelle tracker (0.2 μM) for 5 min. (A) and (E): Fluorescence image of **FVPI** collected red emission channel ($\lambda_{ex}$ = 405 nm, $\lambda_{em}$ = 570–620 nm);(B): Fluorescence image of MitoTracker Deep Red ($\lambda_{ex}$ = 647 nm, $\lambda_{em}$ = 663–738 nm); (F): Fluorescence image of Lyso Tracker Deep Red ($\lambda_{ex}$ = 647 nm, $\lambda_{em}$ = 663–738 nm); (C) and (G) Merged image. (D) and (E): Intensity profile of the region of interest indicated by the white color line. Scale bar = 20 μm

supplied silica gel (mesh 200–300). The solvents primarily used for spectrometry are chromatographic grade solvents.

$^{1}H$ and $^{13}C$ NMR spectra were measured on an AVANCE III digital NMR spectrometer, using tetramethylsilane (TMS) as internal reference; High resolution mass spectrometric (HRMS) analyses were measured on an Agilent 1100 HPLC/MSD spectrometer; Electronic absorption spectra were obtained on a Shimadzu UV-2700 power spectrometer; Photoluminescent spectra were recorded with a HITACHI F4600 fluorescence spectrophotometer with a 1 cm standard

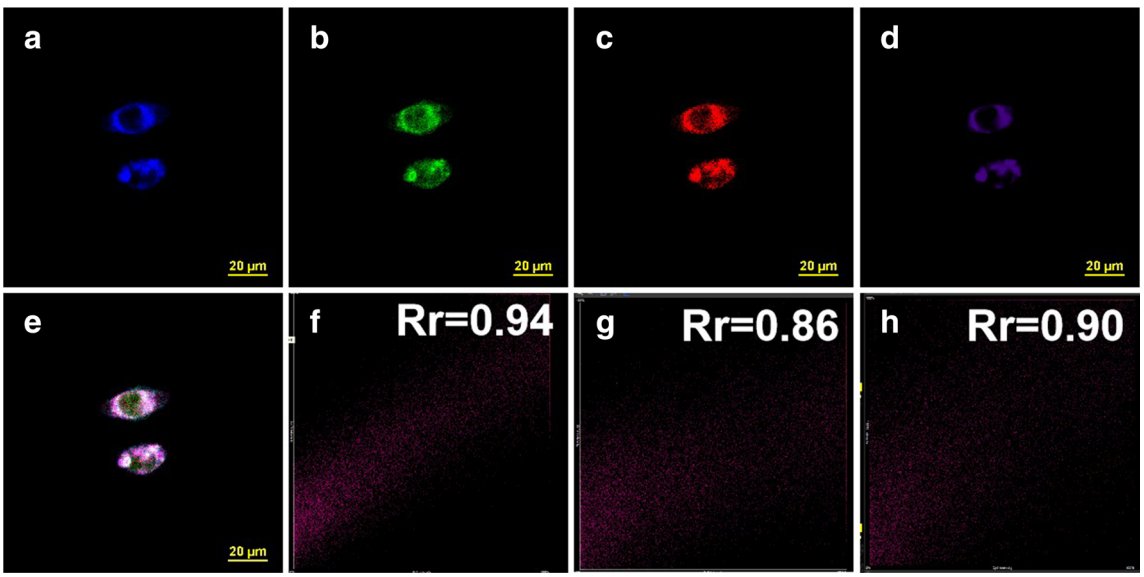


**Fig. 6** Fluorescence image of HeLa cells incubated with **FVPI** (10 μM) for 30 min and MitoTracker Deep Red (0.2 μM) for 5 min. (A) Fluorescence image of **FVPI** collected blue emission channel ($\lambda_{ex}$ = 405 nm, $\lambda_{em}$ = 425–475 nm); (B) Fluorescence image of **FVPI** collected green emission channel ($\lambda_{ex}$ = 405 nm, $\lambda_{em}$ = 500–550 nm); (C) Fluorescence image of **FVPI** collected red emission channel ($\lambda_{ex}$ = 405 nm, $\lambda_{em}$ = 570–620 nm); (D): Fluorescence image of MitoTracker Deep Red ($\lambda_{ex}$ = 647 nm, $\lambda_{em}$ = 663–738 nm); (E) merged image. (F): Correlation plot of **FVPI** and MitoTracker Deep Red intensities with blue emission channels; (G): Correlation plot of **FVPI** and MitoTracker Deep Red intensities with green emission channels; (H): Correlation plot of **FVPI** and MitoTracker Deep Red intensities with red emission channels. Scale bar = 20 μm

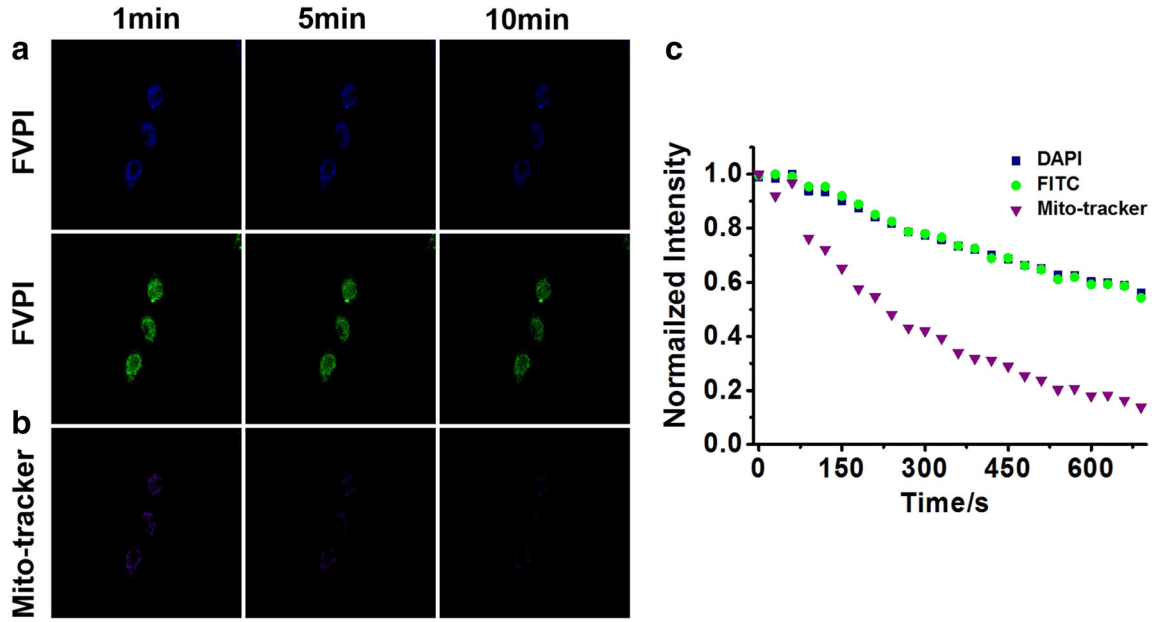


**Fig. 7** (A) Confocal microscopy images of living cells incubated with **FVPI** acquired at different times under successive excitation (DAPI: $\lambda_{ex} = 404$ nm, $\lambda_{em} = 425–475$ nm; FITC: $\lambda_{ex} = 404$ nm, $\lambda_{em} = 500–550$ nm); (B) Confocal microscopy images of HeLa cells treated with MitoTracker Deep Red obtained at definite times ($\lambda_{ex} = 647$ nm, $\lambda_{em} = 663–738$ nm); (C) Normailzed intensities of probe and mito-tracker

quartz cell; Fluorescence imaging of the cells were performed with Nikon AMP1 confocal microscopy. Two-photon imaging was acquired by Nikon AMP1 confocal microscopy.

All fluorescent pictures including fluorescent images and fluorescence intensities in cells were obtained by NIS Elements AR processing software.

## Preparation of Solution of FVPI

Firstly, the **FVPI** was dissolved in N,N-Dimethylformamide to obtain the stock solution (1 mM). The 30 μL stock solution poured into 3 mL various solvents to obtain a solution (10 μM **FVPI**) and it be capable of spectral experiments.

Secondly, the fluorescence quantum yields of **FVPI** were further evaluated by the following eq. (1):

$$\Phi_s = \Phi_r \left(\frac{A_r(\lambda_r)}{A_s(\lambda_s)}\right)\left(\frac{n_s^2}{n_r^2}\right)\frac{F_s}{F_r} \quad (1)$$

*Where the subscripts s and r refer to the sample and the reference, respectively. Φ is quantum yield, F is the integrated emission intensity, A stands for the absorbance, and n is refractive index.*

## Cells Culture and Imaging

The Nankai University (Tianjin, China) provided living cells (HeLa) and fetal bovine serum. Culture medium that can incubate HeLa cells was acquired by Dulbecco's Modified Eagle's Medium (DMEM), 10% fetal bovine serum

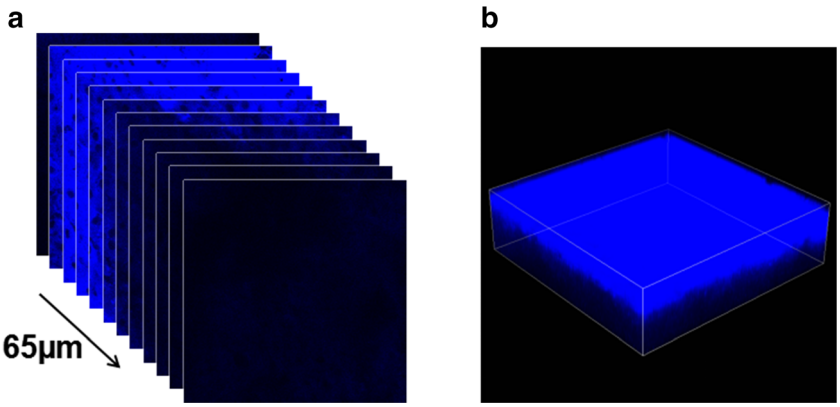


**Fig. 8** TPM fluorescence imaging of the liver tissues incubated with **FVPI** (25 μM) for 60 min. (A and B) 3D fluorescence images ($\lambda_{ex} = 760$ nm, $\lambda_{em} = 425–475$ nm)

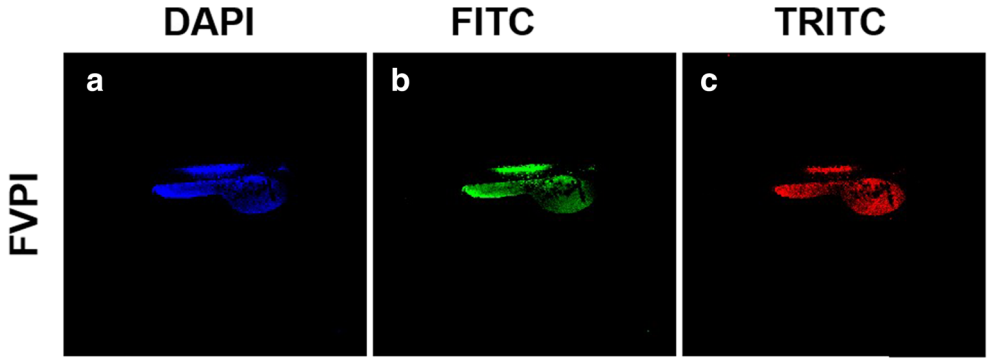


**Fig. 9** Images of zebrafish treated with 10 μM **FVPI**; (A)The blue emission channel ($\lambda_{ex}$ = 405 nm, $\lambda_{em}$ = 425–475 nm); (B) The green emission channel ($\lambda_{ex}$ = 405 nm, $\lambda_{em}$ = 500–550 nm); (C) The red emission channel ($\lambda_{ex}$ = 405 nm, $\lambda_{em}$ = 570–620 nm)

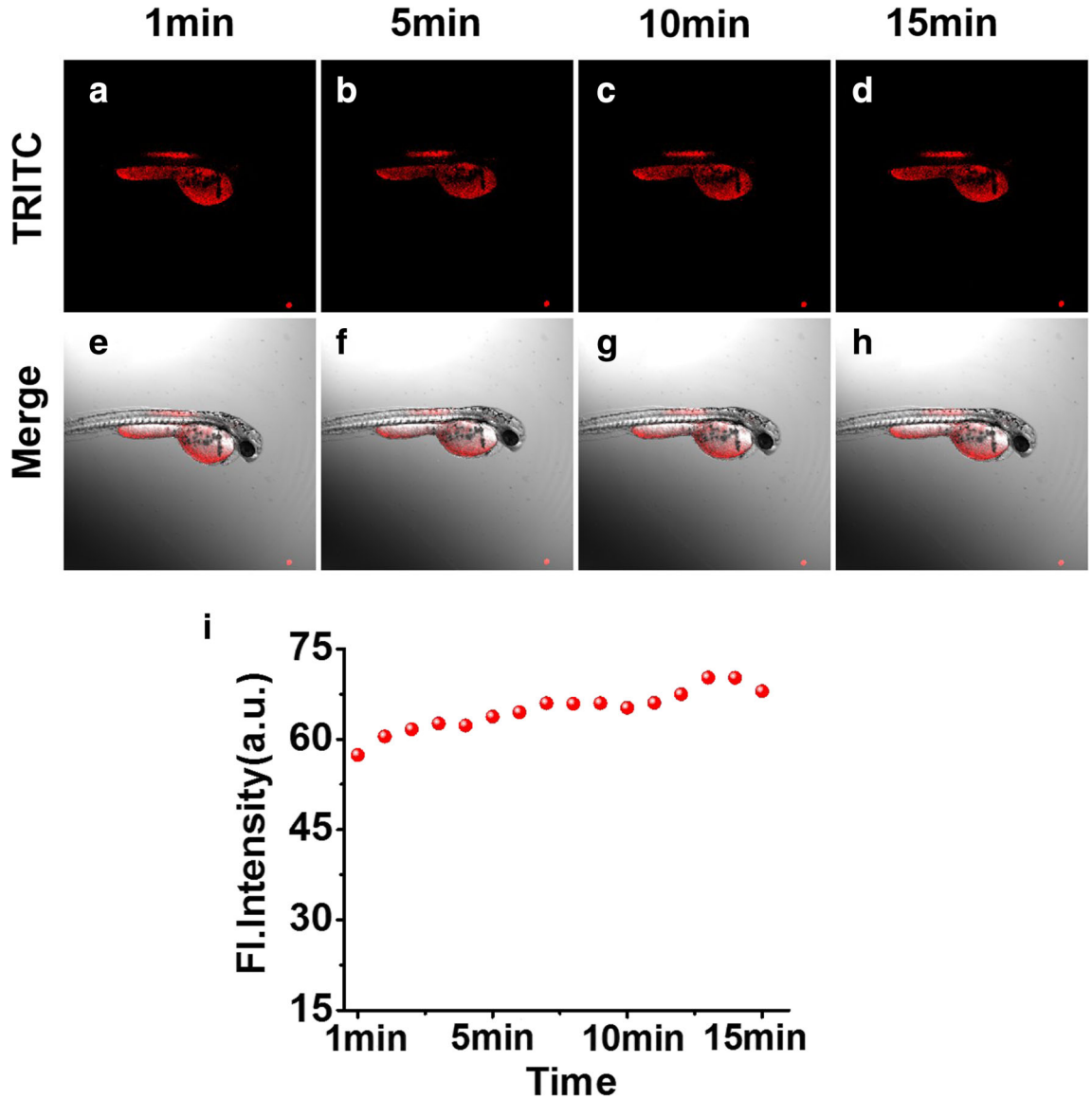


**Fig. 10** Confocal fluorescence images of zebrafish treated with **FVPI** obtained at different times (A-D): Red channel: ($\lambda_{ex}$ = 404 nm, $\lambda_{em}$ = 570–620 nm); (E-H): Merged pictures; (I) Fluorescent intensities of the zebrafish treated with **FVPI** (10 μM) at time points

(FBS) and 5% Antibiotics. Two days before imaging, the living cells were placed on the confocal dish (density of cells was $1 \times 10^5$/ mL) and supplemented 1 ml culture medium. Cells imaging experiment could be performed before the cells reached about 70% coverage. 10 μM **FVPI** were mixed evenly with 1 mL culture medium (pH 7.4) in a tube. The cells were incubated with the above mixed solutions at 37 °C for 0.5 h. Wash cells twice with 1 mL PBS and the fluorescence images were acquired confocal microscopy .

### Co-Colocation Experiment

*Co-colocation experiments were performed in* living HeLa cells. Before performing cell imaging, HeLa cells cultivated in the culture dish according to the way of cell culture in an atmosphere (5% $CO_2$, 95% air) at 37 °C. First, HeLa cells were treated with 10 μM **FVPI** for 0.5 h in an atmosphere (5% $CO_2$, 95% air) at 37 °C, and then the probe were washed using buffer solution after 30 min; Second, HeLa cells were labeled with MitoTracker Deep Red and Lyso-Tracker Deep Red according to the manufacturer's instructions. Third, wash cells twice with 1 mL PBS and the *co-colocation* images were acquired through Nikon AMP1 confocal microscopy.

The probe **FVPI** were excited using a 404 nm laser, and emission was collected between 425 and 475 nm. MitoTracker Deep Red and Lyso-Tracker Deep Red were excited using a 647 nm laser, and emission was collected between 663 and 738 nm.

### Tissues Imaging

Fresh liver tissue was treated with the vibrating-blade microtometo to obtain 400 μm thickness slices; The liver slices were treated with 25 μM **FVPI** in PBS, after incubated 60 min, the liver slices were washed twice by PBS; The tissue slices were placed on the confocal dish. Fluorescence images of tissues were acquired with Nikon AMP1 confocal microscope at Z-scan mode. The tissues fluorescence images were excited using a 760 nm laser, and emission was collected between 425 and 475 nm.

### Zebrafish Imaging

The company (Nanjing Eze-Rinka Biotechnology Co., Ltd) provided Wild type zebrafish. Two days before imaging experiments, the zebrafish was fed at optimal breeding conditions. The zebrafishes were placed on the confocal dish and supplemented 1 ml culture medium. First, the zebrafishes were treated with 10 μM **FVPI** for 0.5 h; Second, the culture medium was removed and further washed twice by PBS; Third, before imaging, the zebrafish was added to new confocal dish and treated with adopted 1% agarose gel. Finally, zebrafish imaging experiment was carried out.

## Results and Discussion

### Optical Properties of the Free Probe

The UV and emission spectra of the dye **FVPI** were investigated in different solvents. The optical data of **FVPI** in diverse solvents were displayed in Fig. 2. For the dye **FVPI**, the consequences exhibited that the compound had maximum absorption and fluorescence peaks at 380 nm and 524 nm in PBS. The probe **FVPI** displayed large Stokes shift (129–147 nm) in organic and pure water systems in Table S2. For more obvious displaying the prove **FVPI** with large Stokes shift, we set out to investigate Stokes shift of **FVPI** in DMF, MeCN, PBS and $H_2O$ (Fig. 3). Thus, the probe **FVPI** with large Stokes shift can avert measurement error and self-quenching in detection process. The standard used Rhodamine 6G ($\Phi = 0.95$) in water and the value of refractive index was 1. Furthermore, the probe **FVPI** showed high fluorescence quantum yield in Table S2.

### Imaging in Living Cells

Before achieving cells images, we have done the cytotoxicity test. The consequences displayed that **FVPI** exhibits low cytotoxicity for HeLa cells (Table S3). The confocal microscopy images (Fig. 4) verified that 10 μM **FVPI** could availably penetrate the cell membrane and enter living HeLa cells. As shown in Fig. 4, **FVPI** emitted bright fluorescence in cytoplasm at three emission channels, and no fluorescence was observed in the extracellular regions. According to the design, the probe was a derivative of pyridine cation, and the pyridine cation was mitochondrial targeting group. So in order to demonstrate that the probe **FVPI** was able to track mitochondria, we further conducted the colocalization experiment.

### Co-Colocation Imaging

Co-localization experiments with commercial organelle dyes were general way for detecting intracellular localization of probes [43]. Therefore, in order to verify the dyes **FVPI** was able to selectively target mitochondria in living cells, co-staining experiments of dyes were implemented. The cells were treated with **FVPI** and the commercial organelle tracker (Mito Tracker Deep Red and Lyso Tracker Deep Red), to demonstrate whether the probe could specifically image mitochondria in living cells. The lightful lilac fluorescence shown in Fig. 5 exhibited the prominent co-localization ability of **FVPI** with MitoTracker Deep Red. The results of using co-staining experiment with

Mito Tracker Deep Red showed high Pearson's colocalization coefficient (Rr = 0.90), nevertheless the Pearson's colocalization coefficient displayed 0.57 when co-stained with Lyso Tracker Deep Red. In order to further prove that the probe can sensitively track mitochondria with three emission colors, we analyzed the experimental data of the three channels in the co-incubation results. The images of incubating Mito Tracker Deep Red strongly suggested that **FVPI** targeted the intracellular mitochondria at three emission channels in Fig. 6 (the Pearson's colocalization coefficient Rr = 0.94 at blue channnel, Rr = 0.86 at green channnel, Rr = 0.90 at red channnel). However, the Pearson's colocalization coefficient was low when the probe incubated with Lyso Tracker Deep Red at three emission channels, respectively (Fig. S1). Thus, **FVPI** predominantly located in the mitochondria in living cells with three emission colors.

Photostability is one of the key indicators for the development of remarkable fluorescent probes [44]. Fluorescence images of **FVPI** and MitoTracker Deep Red were obtained at diverse times under continuous irradiation (Fig. 7). The fluorescence intensity of intracellular dyes was normalized and plotted as a function of time. In Fig. 7, the fluorescence emission of **FVPI** was stable under successive excitation for 11 min. In comparison, at the same laser intensity, the fluorescence intensity of MitoTracker Deep Red decline keenly in 130 s. The above consequence displayed that **FVPI** show high photostability at divese times under continuous excitation.

### Two-Photon Imaging

Compared with one-photon (OP) fluorescent probes, two-photon (TP) fluorescent probes have better bio-sample penetration ability. We have shown that **FVPI** could image mitochondria in HeLa cells at OP excitation. Now, the probe **FVPI** was further study whether own TP property. The HeLa cells were treated with **FVPI** (10 μM) and TP image was implemented by TP fluorescence microscope. As shown in Fig. S2, the extracellular regions were not found fluorescence, the mitochondria was emitted bright fluorescence. The results demonstrated that **FVPI** was able to target mitochondria in canner cells at TP excitation.

The liver tissues were incubated with **FVPI** (25 μM) for 60 min, and then TP microscopy fluorescence images of the slices were acquired at 760 nm excitation and emission was collected between 425 and 475 nm (Fig. 8). As displayed in Fig. 8 A, the phenomenon revealed that the probe can penetrate to tissues depth of 65 μm at TP excitation. The 3D imaging effect of the tissue from superposition of tissue section were further acquired (Fig. 8B). Thus, the result manifested that **FVPI** possessed ability in deep tissues at two-photon excitation.

### Zebrafish Imaging In Vivo

To further evaluate the application of **FVPI** in living system, zebrafish imaging experiment was also conducted. As illustrated in Fig. 9, zebrafish larvae was loaded with (10 μM) **FVPI** for 30 min, and obvious fluorescence could be observed in these samples in three emisssion channels. In Fig. 10, zebrafish stained by **FVPI** exhibited stable fluorescence intensity during continuous laser irradiation of 15 min at red emisssion channel. Furthermore, the experimental results showed that blue emisssion channel and green emisssion channel also had high stability in Fig. S3. These imaging findings demonstrated that **FVPI** could capable of tracking the mitochondria in living system and exist high photostability with three emission colors.

## Conclusion

In summary, we have developed a novel fluorescent probe for imaging mitochondria with three different sets of fluorescence signals based on fluorene cation. The probe could successfully track mitochondria with three different sets of signals. Interestingly, this fluorescence probe exhibited large Stokes shift in different solutions. It is found that **FVPI** showed excellent properties, including high photostability, low cytotoxicity, and two-photon properties. View of the above features, the probe **FVPI** possessed ability tracking mitochondria in the living cancer cells, tissues and zebrafish. This finding will provide a new platform for the constructing mitochondria-targetable fluorescent probes with excellent optical properties.

**Acknowledgements** Funding was partially provided by NSFC (51973082, 21472067, 51503077, 21672083, 21877048); Taishan Scholar Foundation (TS 201511041), doctor start up fund of University of Jinan (XBS1512), NSFSP (ZR2015PE001), and the startup fund of the University of Jinan (309-10004).

## References

1. Chinta LV, Lindvere L, Dorr A, Sahota B, Sled JG, Stefanovic B (2012) Quantitative estimates of stimulation-induced perfusion response using two-photon fluorescence microscopy of cortical microvascular networks. Neuroimage 61:517–524
2. Folmes CD, Dzeja PP, Nelson TJ, Terzic A (2012) Mitochondria in control of cell fate. Circ Res 110:526–529
3. Brookes PS, Levonen AL, Shiva S (2002) Mitochondria: regulators of signal transduction by reactive oxygen and nitrogen species. Free Radic Biol Med 33:755–764
4. Gutierrez J, Ballinger SW, Darley-Usmar VM (2006) Free radicals, mitochondria, and oxidized lipids: the emerging role in signal transduction in vascular cells. Circ Res 99:924–932

5. Lemasters JJ, Hackenbrock CR (1978) Firefly luciferase assay for ATP production by mitochondria. Methods Enzymol 57:36–50
6. Eavaro F, Ramachandran A, Mccormick R (2010) MicroRNA-210 regulates mitochondrial free radical response to hypoxia and Krebs cycle in Cancer cells by targeting Iron sulfur cluster protein ISCU. PLoS One 5:10345
7. Lee D, Jung MK, Yin J, Kim G, Pack CG, Yoon J (2017) An aniline bearing hemicyanine derivative serves as a mitochondria selective probe. Dyes Pigments 136:467–472
8. Nunnari J, Suomalainen A (2012) Mitochondria: in sickness and in health. Cell 148:1145–1159
9. Chang DT, Reynolds IJ (2006) Differences in mitochondrial movement and morphology in young and mature primary cortical neurons in culture. Neuroscience 141:727
10. Garber AJ, Salganicoff L (1973) Regulation of oxalacetate metabolism in liver mitochondria. J Biol Chem 248:1520
11. Hunter D, Haworth R (1979) The $Ca^{2+}$-induced membrane transition in mitochondria. Arch Biochem Biophys 195:468–477
12. Du H, Guo L, Yan S, Sosunov AA, Mckhann GM, Yan SD (2010) Early deficits in synaptic mitochondria in an Alzheimer's disease mouse model. P Natl Acad Sci USA 107:18670–18675
13. Hoye AT, Davoren JE, Wipf P, Fink MP, Kagan VE (2008) Targeting mitochondria, accounts Chem. Res. 41:87–97
14. Dickinson BC, Chang CJ (2011) Chemistry and biology of reactive oxygen species in signaling or stress responses. Nat Chem Biol 7: 504–511
15. Cassarino DS, Jr BJ (1999) An evaluation of the role of mitochondria in neurodegenerative diseases: mitochondrial mutations and oxidative pathology, protective nuclear responses, and cell death in neurodegeneration. Brain Res Rev 29:1–25
16. Oberley LW (1998) Mitochondria and free radicals in neurodegenerative diseases. Trends Neurosci 21:131–132
17. Warda M, Kim HK, Kim N (2013) A matter of life, death and diseases: mitochondria from a proteomic perspective, expert rev. Proteomics 10:97–111
18. Neto BAD, Corrêa JR, Silva RG (2013) Selective mitochondrial staining with small fluorescent probes: importance, design, synthesis, challenges and trends for new markers. RSC Adv 3:5291–5301
19. Jr AO, Johansson HE, Ruth JL (2011) Stellaris™ fluorescence in situ hybridization (FISH) probes: a powerful tool for mRNA detection, Nat. Methods 8: i-ii
20. Drummen GP (2012) Fluorescent probes and fluorescence (microscopy) techniques–illuminating biological and biomedical research. Molecules 17:14067–14090
21. Chen H, Tang Y, Lin W (2016) Recent progress in the fluorescent probes for specific imaging small molecular weight thiols in living cells, trends anal. Chem. 76:166–181
22. Srikun D, Albers AE, Nam CI (2010) Organelle-targetable fluorescent probes for imaging hydrogen peroxide in living cells via SNAP-tag protein labeling. J Am Chem Soc 132:4455–4465
23. Shim SH, Xia C, Zhong G (2012) Super-resolution fluorescence imaging of organelles in live cells with photoswitchable membrane probes. P Natl Acad Sci USA 109:13978–13983
24. Sednev MV, Belov VN, Hell SW (2015) Fluorescent dyes with large stokes shifts for super-resolution optical microscopy of biological objects: a review, methods Appl. Fluoresc. 3:042004
25. Liu X, Qi F, Su Y, Chen W, Yang L, Song X (2016) A red emitting fluorescent probe for instantaneous sensing of thiophenol in both aqueous medium and living cells with a large stokes shift. J Mater Chem C 4:4320–4326
26. Feng W, Li M, Sun Y, Feng G (2017) Near-infrared fluorescent turn-on probe with a remarkable large stokes shift for imaging Selenocysteine in living cells and animals. Anal Chem 89:6106
27. Lin W, Yuan L, Cao Z, Feng Y, Song J (2010) Through-bond energy transfer cassettes with minimal spectral overlap between the donor emission and acceptor absorption: coumarinrhodamine dyads with large pseudo-stokes shifts and emission shifts. Angew Chem Int Ed Eng 49:375–379
28. Xu W, He L, Qi X (2018) A far-red-emissive AIE active fluorescent probe with large stokes shift for detection of inflammatory bowel disease in vivo. J Mater Chem B 6:2–7
29. Yuan L, Lin W, Chen H (2013) Analogues of Changsha near-infrared dyes with large stokes shifts for bioimaging. Biomaterials 34:9566–9571
30. Wu WL, Wang ZY, Xi D (2016) An effective colorimetric and ratiometric fluorescent probe based FRET with a large Stokes shift for bisulfite. Sci Rep 6:25315
31. Zielonka J, Joseph J, Sikora A, Hardy M, Ouari O, Vasquez-Vivar J, Cheng G, Lopez M, Kalyanaraman B (2017) Mitochondria-targeted Triphenylphosphonium-based compounds: syntheses, mechanisms of action, and therapeutic and diagnostic applications. Chem Rev 117:10043–10120
32. Smith RAJ, Hartley RC, Murphy MP (2011) Mitochondria-targeted small molecule therapeutics and probes. Antioxid Redox Signal 15: 3021–3038
33. Pak YL, Li J, Ko KC, Kim G, Lee JY, Yoon J (2016) Mitochondria-targeted reaction-based fluorescent probe for hydrogen sulfide. Anal Chem 88:5476–5481
34. Kawazoe Y, Shimogawa H, Sato A, Uesugi M (2011) A mitochondrial surface-specific fluorescent probe activated by bioconversion. Angew Chem Int Ed 50:5478–5481
35. Guo DL, Chen T, Ye DJ, Xu JY, Jiang HL, Chen KX (2011) Cell-permeable iminocoumarine-based fluorescent dyes for mitochondria. Org Lett 13:2884–2887
36. Dickinson BC, Chang CJ (2008) A targetable fluorescent probe for imaging hydrogen peroxide in the mitochondria of living cells. J Am Chem Soc 130:9638–9639
37. Xu Q, Heo CH, Kim JA, Lee HS, Hu Y, Kim D (2016) A selective imidazoline-2-thione-bearing two-photon fluorescent probe for hypochlorous acid in mitochondria. Anal Chem 88:6615–6620
38. Lee MH, Park N, Yi C, Han JH, Hong JH, Kim KP (2014) Mitochondria-immobilized pH-sensitive off-on fluorescent probe. J Am Chem Soc 136:14136–14142
39. Wang L, Yuan L, Zeng X, Peng J, Ni Y, Er JC (2016) A multisite-binding switchable fluorescent probe for monitoring mitochondrial ATP level fluctuation in live cells. Angew Chem Int Ed 55:1773–1776
40. Ren M, Deng B, Zhou K, Kong X, Wang J, Lin W (2017) A single fluorescent probe for dual-imaging viscosity and H2O2 in mitochondria with different fluorescence signals in living cells. Anal Chem 89:552–555
41. Meng F, Liu Y, Niu J, Lin W (2017) A novel fluorescent probe with a large stokes shift for real-time imaging mitochondria in different living cell lines. Tetrahedron Lett 58: 3287–3293
42. He L, Liu X, Zhang Y, Yang L, Fang Q, Geng Y, Chen W, Song X (2018) A mitochondria-targeting ratiometric fluorescent probe for imaging hydrogen peroxide with long-wavelength emission and large stokes shift. Sensors Actuators B Chem 276:247–253
43. Yang W, Chan PS, Chan MS, Li KF, Lo PK, Mak NK, Cheah KW, Wong MS (2013) Two-photon fluorescence probes for imaging of mitochondria and lysosomes. Chem Commun 49:3428–3430
44. Haack RA, Swift KM, Ruan Q, Himmelsbach RJ, Tetin SY (2017) The photostability of the commonly used biotin-4-fluorescein probe. Anal Biochem 531:78–82


**Publisher's Note** Springer Nature remains neutral with regard to jurisdictional claims in published maps and institutional affiliations.